7.07 The Dynamics and Convective Evolution of the Upper Mantle

E. M. Parmentier, Brown University, Providence, RI, USA

7.07.1 Introduction

The thermal structure of the oceanic upper mantle plays an important role in the larger-scale dynamics of the mantle. Fortunately, this region of the Earth is one that is accessible to observation by a variety of geophysical tools and so can provide a basis for understanding solid-state convective instability, with implications for even more general settings than the Earth's upper mantle. It can be argued that the Earth's upper mantle is the best natural laboratory available to us to study the convective evolution of planetary interiors.

The goal of this chapter is to summarize current understanding of the evolution of the upper mantle based on observations and theoretical predictions, beginning with some of the earliest observations on how cooling the mantle from above would be expressed in seafloor depth, heat flow, and geoid height as functions of age. It is not possible to consider the role of convective instability in the upper mantle in isolation from other forms of larger-scale mantle flow. While no general agreement has yet emerged on how various scales of convection may affect the upper mantle, small-scale thermal convective instability generated within the upper mantle provides a viable explanation for many important observations. Convection in the upper mantle may be driven by buoyancy resulting both from cooling at the surface and by melting. Mantle cooling is expressed in oceanic heat flow and in geoid height and seafloor depth through the effect of cooling on mantle density.

Buoyancy due to melting may be expressed in intraplate volcanism. Only a few long-lived, age progressive, linear volcanic chains meet all the criteria of the deep-mantle plume-fixed hot-spot hypothesis. Decompression melting in small-scale thermally driven convective upwellings has been one favored explanation for volcanic ridges aligned with plate motion. Seafloor volcanism may also reflect spontaneously generated instability driven by decompression melting, which has been termed 'magmatic convective storms'. Buoyant decompression melting beneath moving plates is a possible mechanism for the abundant short-lived island chains and volcanic ridges identified on the Earth's seafloor.

Finally, the role of mantle upwelling and melting beneath spreading centers is important to consider, in part because it is responsible for the generation of the oceanic crust and is a factor controlling spreading center structure. However, melting and melt extraction under spreading centers leave behind residual mantle that is transported away from the spreading center. Compositional changes are expected to affect viscosity or creep rate and create a stable chemical stratification, thus fundamentally influencing convective instability everywhere in the upper mantle (Chapter 2.14).

7.07.2 Cooling the Mantle from Above

7.07.2.1 A Historical Perspective

Turcotte and Oxburgh (1967) identified the moving lithospheric plates (Chapter 6.02) as the conductive thermal boundary layer at the top of mantle convection cells, thus establishing a physical relationship between upper-mantle thermal structure and mantle dynamics. During the emergence of plate tectonics, measurements of seafloor depth and heat flow in the oceans provided the first direct evidence on the thermal structure of the upper mantle. Heat flow generally decreased with crustal age but showed great variability, particularly at young ages. This variability is now understood to be due primarily to hydrothermal circulation of seawater through permeable crustal rocks. In contrast, seafloor depths showed a much more systemic variation with seafloor age. The age dependence of isostatic seafloor depth, which depends on the depth-averaged temperature, was recognized as a stronger observational constraint than heat flow on upper-mantle thermal structure (Langseth *et al.*, 1966; McKenzie, 1967; Vogt and Ostenso, 1967; McKenzie and Sclater, 1969; Sleep, 1969).

The thermal structure that develops due to conductive cooling should be, at least to first order, only a function of crustal age, rather than an independent function of both distance from spreading center and plate velocity. Observations of seafloor depth and age generally confirmed this age dependence. The Turcotte and Oxburgh boundary layer hypothesis, in the simple form suggested originally, indicated that the thermal boundary layer should continue to thicken as the square root of age so that old seafloor would continue to subside. This did not appear to explain observations showing a relatively uniform depth of old seafloor which required that the thermal boundary layer evolve to a nearly constant thickness. Models for upper-mantle thermal structure that were consistent with average depth of seafloor as a function of age from the growing collection of observations treated the conductive cooling of horizontally moving upper mantle, as in the simple boundary layer theory, but with the added assumption of a uniform temperature at a prescribed depth (Langseth *et al.*, 1966; McKenzie, 1967). A relatively uniform seafloor depth at old ages requires a mechanism to transport heat to bottom of the thermal boundary layer, thus reducing the rate at which it thickens. This set the stage for research in the following several decades and is still a source of continuing study and debate.

7.07.2.2 Convective Instability versus Heating by Hot Spots – Depth–Age and Heat flow

Both small-scale convective instability of the cool thermal boundary and heating at hot spots (*see* Chapters 1.13 and 7.09) may play a role in transporting heat to the bottom of the thermal boundary layer, but no general consensus has yet emerged on a single mechanism of heating that can explain all available observations. Ideally, observed variations in seafloor depth might constrain the relative importance of these two mechanisms, but such interpretations are limited by the relatively small amount of old seafloor with a well-determined age and by the uncertainty in correcting for the thickness and load of sediments. Simply averaging all depth measurements at a given age indicates that old seafloor is, on average, shallower than would be predicted by conductive cooling alone. Johnson and Carlson (1992; see also Carlson and Johnson (1994)) report a recent assessment of this averaged depth–age relationship using data at sites where drilling has reached basement and for which the age is well determined. As shown in **Figure 1**, old seafloor appears, on average, to be at least several hundred meters shallower than the depth predicted by the purely conductive cooling models that fits very well at relatively young ages. So the question is why old seafloor is often shallower than predicted by conductive cooling and how we might infer the physical processes responsible.

Heating due to hot spots should correlate with the length of time that a given piece of seafloor has spent in the proximity of a hot spot (Crough, 1975).

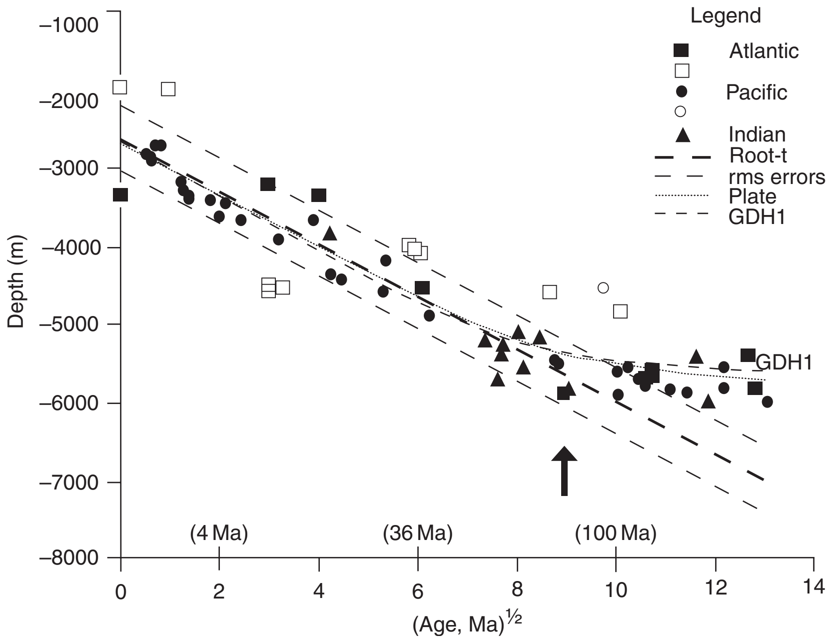

Figure 1 Depth–age for various oceans, based on sediment and crustal thickness corrected seafloor depths (Johnson and Carlson, 1992), compared to conductive half-space, and plate models with 120 km thick plate and 1350 °C mantle temperature (the plate model) and a 95 km thick plate and 1450 °C mantle (the GDH1 model).

Heestand and Crough (1981) sorted the depth of seafloor in the North Atlantic by distance from the nearest hot-spot track. Comparing depth–age for seafloor in constant distance ranges indicated no flattening at old ages. In the South Atlantic, where hot-spot influences should be less significant, Hayes (1988) noted that depth followed a purely conductive cooling curve to ages approaching 120 My, but noted the complication of a persistent asymmetry in apparent subsidence rate across the spreading axis. An asymmetry in apparent subsidence rate was also found in the Southeast Indian Ocean (Hayes, 1988) and across the East Pacific Rise (EPR) (Eberle and Forsyth, 1995). One possibility may be that this asymmetry reflects the dynamic topography of larger-scale mantle flow on which the depth–age subsidence is superimposed (*see* Chapter 6.05).

The Pacific Plate contains not only relatively large areas of old seafloor but also numerous seamounts and hot-spot tracks (e.g., Wessel and Lyons, 1997). Schroeder (1984) compiled depth–age data for the Pacific. Eliminating data within 800 km of hot-spot tracks resulted in a good correlation of depth with square root of age for ages less than 80 My. All seafloor older than 80 My was shallower than predicted by conductive cooling alone and was within 800 km of hot spots or hot-spot tracks. Renkin and Sclater (1988) analyzed the effect of uncertainties in basement age and sediment thickness on depth–age correlations in the North Pacific. Arguing that volcanic constructs always result in shallower seafloor, they proposed that modal seafloor depth, or more precisely a range enclosing two-thirds of the measured depths at any age, provides an estimate of subsidence associated with cooling least biased by volcanism. Modal depths increase with age more slowly than predicted by conductive cooling for ages exceeding about 80 My. Plotting modal depths with age along a corridor of Pacific seafloor containing several swell-like features, Renkin and Sclater argue that not even the deepest depths fall along a conductive cooling model.

Small-scale convective instability of the thermal boundary layer, in addition to hot spots, may advectively transport heat to the bottom of the conductive boundary layer. The possible importance of small-scale convection was first suggested on the basis of averaged depth–age curves that deviate from purely conductive cooling at a seafloor age of about 70–80 My, which was presumed to correspond to the onset of convective instability (Parsons and McKenzie, 1978). Beyond this age, convective heat transfer was thought to maintain the nearly constant thermal boundary layer thickness implied by the plate model (Davis and Lister, 1974; Parsons and Sclater, 1977; Stein and Stein, 1992). Plate thickness must be consistent with the heat flow measured on old seafloor (Davis *et al.*, 1984; Lister *et al.*, 1990; Nagihara *et al.*, 1996), as well as its depth. **Figure 2** from Nagihara *et al.* (1996) shows heat flow values for old seafloor in the northwestern Pacific and in the western North Atlantic, both areas where high-quality heat flow and data needed to correct depth for sediment loading and crustal thickness variations are available. Also shown are predictions from two versions of the plate model and purely conductive cooling, all of which are thought to provide reasonable fits to the depth–age relationship of younger seafloor. Heat flow is higher and seafloor is consistently shallower than predicted by conductive cooling. The plate model of parameters of Parsons and Sclater (1977) with a plate thickness 125 km and a mantle temperature 1350°C fits the depths well but underestimates the heat flow. In contrast, the hotter and thinner plate model of Stein and Stein (1992) with a plate thickness 95 km and a mantle temperature 1450°C fits the heat flow well but underestimates old seafloor depth. It is worth noting that this mantle temperature is significantly higher than that estimated from melting in adiabatically upwelling mantle beneath presently active spreading centers, frequently inferred to be 1325–1350°C.

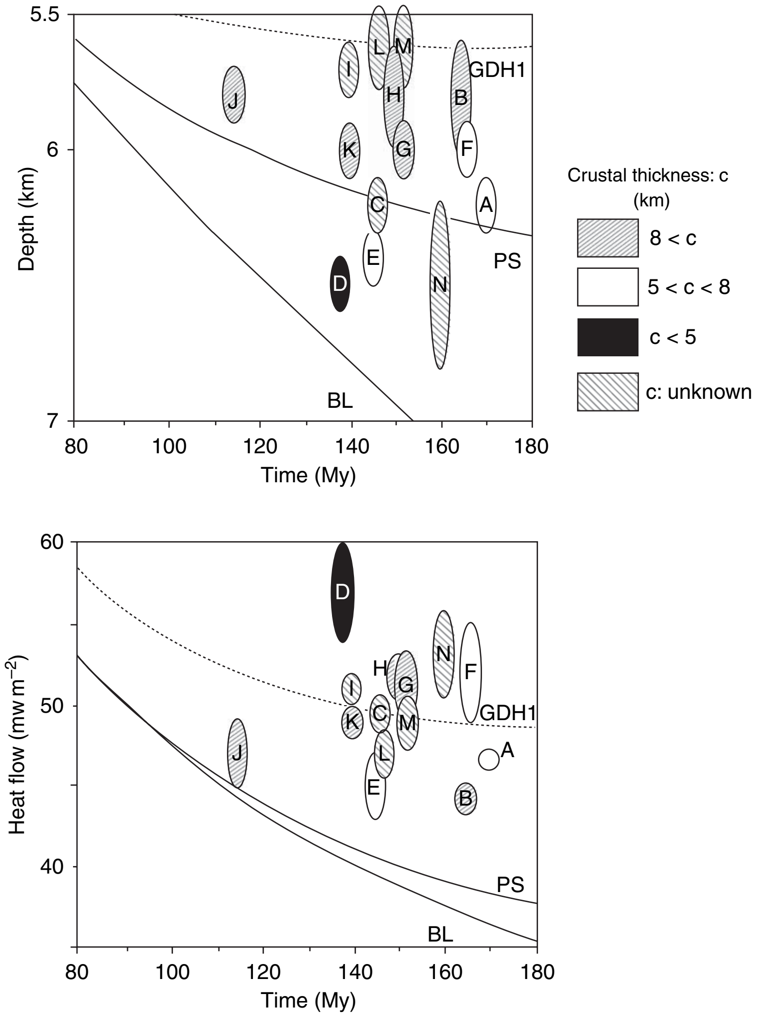

Figure 2 Seafloor basement depth, corrected for sediment load and crustal thickness where available (top) and heat flow (bottom) at sites in the western North Pacific (A–F) and northwestern Atlantic (G–N) as functions of age from Nagihara *et al.* (1996). The location of specific sites is identified in table 1 and figure 1 of Nagihara, *et al*. Model curves for the plate models (PS and GDH1) and half-space cooling (BL).

7.07.2.3 Geoid Height as a Measure of Upper-Mantle Thermal Structure

As discussed above, the earliest interpretations of the thermal evolution of the upper mantle relied largely on heat flow and isostatic seafloor depth, with the isostatic assumption justified by the absence of free-air gravity anomalies correlated with the depth–age variation. Following the advent of sea-surface elevation measurements from satellite altimetry, the long wavelength geoid (Chapter 3.02) and gravity provided further constraint on upper-mantle thermal structure (Chase, 1985; Smith, 1998). Isostatic seafloor depth measures the density averaged over depth in the mantle; geoid height measures the first moment of the density distribution with depth (Haxby and Turcotte, 1978). Conductive cooling predicts that geoid height decreases linearly with age (Haxby and Turcotte, 1978) as they observed along a Geos3 altimetry track in the North Atlantic. Also using early Geos3 altimetry data, Sandwell and Schubert (1980) found that geoid height decreases approximately linearly with seafloor age for ages less than about 80 My in the Atlantic and southeast Indian spreading centers with geoid slopes in the range –0.131 to –0.149 m My^{-1}, generally consistent with a conductive cooling thermal boundary layer. In constrast, the geoid height predicted by the plate model should flatten over old seafloor. Sandwell and Schubert (1980) found that geoid height in the southeast Pacific was not consistent with a simple linear geoid–age relationship, but decreased rapidly with age. The decrease was much more rapid than predicted by the plate model used to explain flattening of old seafloor. This is further discussed below.

The geoid height is sensitive to density variations over much larger distances than gravity anomalies. Therefore, density variations throughout the Earth, not just in the upper mantle, contribute to geoid height variations. The difficulty in using geoid as a constraint on the age dependence of the upper mantle is to separate variations in geoid height with seafloor age from other contributions, for example, from oceanic swells or hot spots. One approach to filtering out the long wavelength contributions is to measure the change in geoid height across fracture zones which juxtapose seafloor of different ages (Crough, 1979a; Detrick, 1981). If geoid height decreases linearly with age as expected for conductive cooling, the change in geoid height across a fracture zone of constant age offset should remain constant as seafloor on each side of the fracture zone ages. In constrast, the plate model should show a change in geoid height across the fracture zone that decreases with age and which vanishes once thermal boundary layer thickness becomes constant. Observations suggest that geoid slope decreases with age, but it appears to do so at a much earlier age than that at which the seafloor flattens. Studies of variations of geoid height with age include Cazenave (1984), Driscoll and Parsons (1988), and Freedman and Parsons (1990). Geoid height as a function of age from Cazenave (1984), plotted as geoid–age slope, is shown in **Figure 3**.

Determining the geoid height change with age using measurements across fracture zones is elegant in concept but difficult in practice. Mechanical behavior of lithosphere, both plate flexure associated with differential subsidence (Sandwell and Schubert, 1982a, 1982b) and thermal bending (Parmentier and Haxby, 1985; Wessel and Haxby, 1990), create uncompensated seafloor topography over distances of 50–100 km adjacent to fracture zones. The resulting geoid anomalies may obscure the identification of the change in isostatic geoid height. Even given these

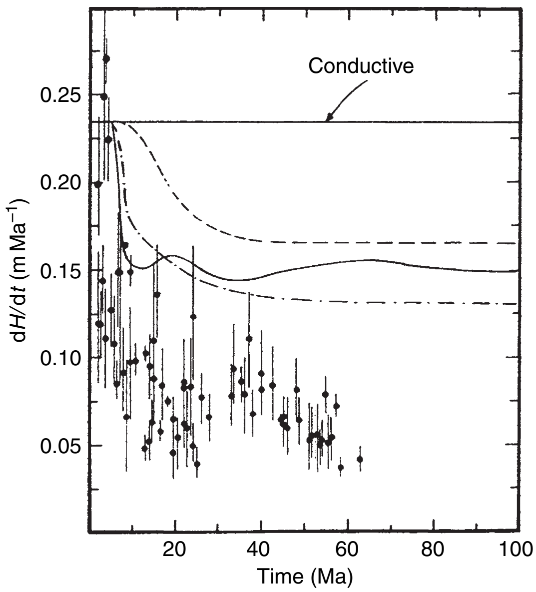

Figure 3 Geoid–age slope as a function of age with data from Cazenave (1984). Pure conductive cooling leads to the constant geoid–age slope as shown. The observations indicate a rapid decline with age. Curves show model predictions from Buck and Parmentier (1986) for convective cooling with an activation energy of 420 kJ mol^{-1} and an activation volume of 10 $cm^3\,mol^{-1}$. Dashed and long-short dashed curves are for a model reference viscosity of 10^{18} and 5×10^{18} Pa s, respectively. The solid curve is also for a 10^{18} Pa s viscosity but in a wider and more finely discretized model domain.

uncertainties, geoid height variation with age is not explained by either the half-space cooling or the plate model mantle thermal structure.

7.07.2.4 Seismic Velocity and Attenuation as Measures of Upper-Mantle Structure and Flow

The age dependence of the apparent elastic thickness of the oceanic lithosphere might also constrain the variation of mantle thermal structure with age. While the focal depths of oceanic intraplate earthquakes increase with age following a 650–700°C isotherm in a conductive cooling model (Bergman and Solomon, 1984; Weins and Stein, 1984), most of the seismicity reported occurs at ages less than 70 My. Flexure of lithosphere at trenches should also reflect the mechanical thickness. Levitt and Sandwell (1995) indicate that plate thickness increases with age of subducting lithosphere and that the plate in the Stein and Stein (1992) thermal model may be too hot and thin. However, the data do not resolve the difference between simple conductive cooling and a plate model with a thicker plate.

Seismic velocities and attenuation in the upper mantle (Chapters 1.16 and 1.17) also constrain thermal structure and its age evolution. Surface wave dispersion has been used to infer the velocity variation with age and depth (Nishimura and Forysth, 1989; Ritzwoller *et al.*, 2004; Priestley and McKenzie, 2006; Maggi *et al*, 2006; Weeraratne *et al.*, 2007; Zhou *et al.*, 2006). As shown in **Figure 4**, seismic shear-wave velocities in the upper mantle generally decrease with depth at a given age and increase with age at a given depth. Seismic velocities continue to change with age at depths exceeding 150 km. This change, if attributable to temperature, clearly contradicts the plate model which implicitly assumes that mantle temperature at depths greater than the plate thickness do not change with age.

Seismic velocity distributions like those in **Figure 4** they may also constrain the depth to which convective instability has cooled the mantle. Early studies like that of Nishimura and Forsyth (1989) probably do not resolve variations deeper than ~200 km. More recent studies using longer period (and consequently longer wavelength) surface waves (Maggi *et al.*, 2006; Zhou *et al.*, 2006), which should resolve velocity variations to greater depth, indicate variations deeper than 200 km. However, the extent to which these variations correlate with plate age has not been established.

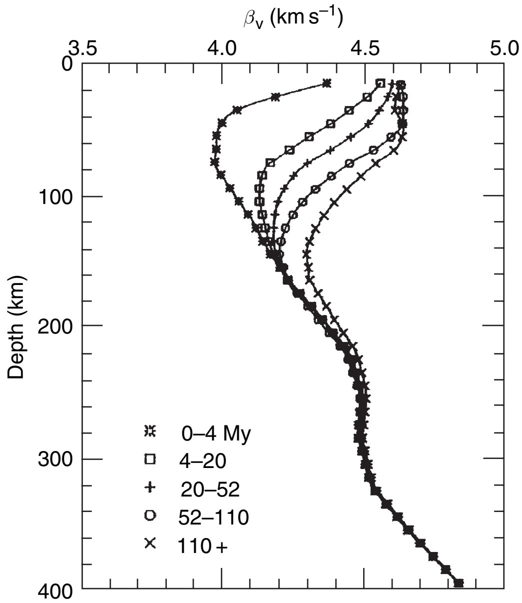

Figure 4 Vertically polarized shear-wave velocity in the Pacific as a function of depth in various age intervals determined from Rayleigh wave dispersion (Nishimura and Forsyth, 1989). Note that shear-wave velocity changes with age at depths greater than would be consistent with a plate model that fits the depth–age relationship (≤125 km). Changes with age continue beneath seafloor with ages exceeding 110 My.

Since the pressure, or depth, of phase changes in the upper mantle (Chapter 2.06) depends on temperature, temperature variations should be reflected in variations in the thickness of the mantle transition zone. Using travel times of converted phases and SS precursors, the results of Lawrence and Shearer (2006; figure 6b) show systematic westward thickening of the transition zone in the Pacific, correlating with increasing plate age. This could imply temperature variations associated with convective instabilities beneath cooling plates may extend to depths of at least the top of the transition zone, ~440 km deep.

The origin of the seismically defined low-velocity, high-attenutation asthenosphere is not fully resolved (Chapter 2.02). The possible effects of small amounts of melt (Chapter 2.18) have been frequently invoked but recent studies indicate that the presence of melt may not be required (Stixrude and Lithgow-Bertelloni, 2006; Priestley and McKenzie, 2006), based on new understanding of the factors controlling shear-wave velocities at seismic frequencies now emerging. Stress relaxation at grain boundaries is thought to be an important anharmonic effect that introduces a frequency–grain size variation and a temperature dependence to the elastic moduli in addition to that of high-frequency (harmonic) variations with temperature and pressure (Gribb and Cooper, 1998; Faul and Jackson, 2005). Grain-size variations could thus contribute to the velocity variation with depth like those shown in **Figure 4**. Using the parametrizations of Priestley and McKenzie (2006) as a first attempt to assess the role of temperature alone, the velocity change of 0.1 km s^{-1} at 150 km depth between 52 and 110 My and >110 My would require cooling in the range of 100–200°C.

Seismic anisotropy (*see* Chapter 2.16) in the upper mantle also provides a possible indication of mantle flow. Azimuthal anisotropy has been long recognized (cf. Nishimura and Forsyth, 1989), but its depth variation and the relative contributions from the lithosphere and asthenosphere are not yet resolved. In a simple unidirectional parallel flow, the seismic fast direction is usually assumed to lie close to the shear plane and in the flow direction. In more complex flows, seismically fast direction has been assumed to coincide with the local direction of maximum accumulated elongation. However, the strength and local direction of anisotropy will be determined by the rates at which preferred orientation of mineral grains is created and destroyed by shear and dynamic recrystallization, respectively (Kaminski and Ribe, 2001, 2002; Wenk and Tomé, 1999; Chastel *et al.*, 1993). Several recent global tomography studies have also reported radial anisotropy that is more pronounced beneath the Pacific Plate than elsewhere in the oceanic upper mantle (e.g., Ekstrom and Dziewonski, 1998; Gaboret *et al.*, 2003). Could this radial anisotropy be a consequence of seismically fast directions vertically aligned in the upwellings and downwellings of convective motion? Hopefully, questions of this type can be resolved by continuing study.

7.07.2.5 Upper-Mantle Electrical Conductivity – Water Content and Temperature

Long-period magnetotelluric studies of mantle electrical structure beneath the eastern North Pacific Ocean can detect electrical conductivity structure between 150 and 1000 km (Lizarralde *et al.*, 1995). Interpretation of this data reveals a conductive zone between 150 and 400 km depth with continuously decreasing conductivity at greater depth. Mantle conductivity in this region is comparable to that in the Basin and Range Province and much higher than that in the Canadian Shield. High conductivities could be explained by the presence of gravitationally stable partial melt. Alternatively, conductivity estimates on measurements of hydrogen solubility and diffusivity in olivine can explain the high conductivities observed. This reinforces the possible role of water in controlling the physical properties, and particularly the rheology, of the upper mantle (Hirth and Kohlsedt, 1996; Hirth *et al.*, 2000). Several recent studies measuring the electrical conductivity of wet olivine (Yoshino *et al.*, 2006; Wang *et al.*, 2006) reach opposing conclusions on whether intragranular water (H-defects) alone can explain observed conductivities or whether partial melt is required.

7.07.2.6 The Age of Thermal Convective Instability beneath Oceanic Lithosphere

In global gravity anomaly maps (Chapter 3.02) derived from Seasat altimetry data, Haxby noticed gravity lineations in the Pacific with 150–200 km wavelength aligned in the direction of plate motion as shown in **Figure 5**. Haxby and Weissel (1986) suggested that these gravity lineations were a consequence of mantle convection currents organized by plate motions. In a sheared fluid layer with an initial linear temperature gradient, corresponding to heating from below and cooling from above, Richter (1973) and Richter and Parsons (1975) showed that convective instability should take the form of convective rolls aligned with shearing due to plate motion. The presence of gravity lineations due to convective instability beneath lithosphere only a few million years old contrasted with the view that convective instability at ages ~70 My explained the flattening of old seafloor.

Motivated by the observed gravity anomalies, numerical solutions for steady-state finite amplitude thermal convection showed that convective instability at young ages could be consistent with mantle thermally activated creep rheology (Buck, 1985) and estimated the convective heat fluxes required to explain the observed gravity anomalies (Lin and Parmentier, 1985). Numerical solutions for the development of thermal convection in a fluid layer cooled from above, with a plausible range of rheological parameters, predicted the effect of convective instability on geophysical observables (Buck and Parmentier, 1986). This study assumed that stresses generated by cool mantle sinking from the bottom of the unstable thermal boundary layer did not contribute to seafloor topography and resulting geoid

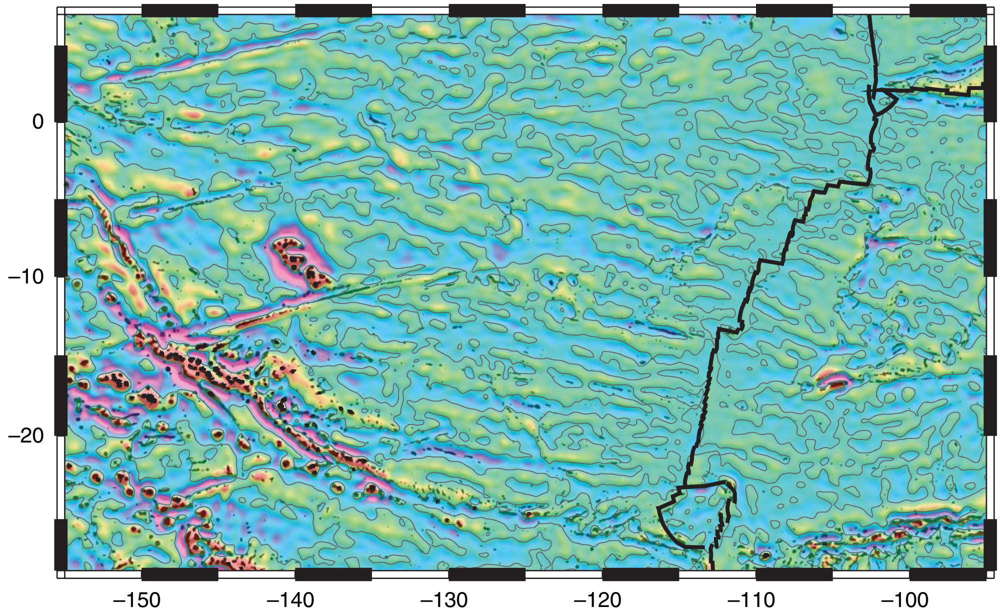

Figure 5 Haxby gravity lineations dipicted in this satellite gravity image by Sandwell and Fialko (2004). Band-pass filtered gravity anomaly (80 km < λ < 600 km) derived from retracked satellite altimeter data. Color scale saturates at $\pm$15 mGal. Gravity lineaments with 140 km wavelength develop between the ridge axis and 6 Ma and are oriented in the direction of absolute plate motion. Lineaments on older seafloor have somewhat longer wavelength ($\sim$180 km) and cross the grain of the seafloor spreading fabric. Gravity lineaments also occur on the plate to the east of the East Pacific Rise.

anomalies, implying that this negatively buoyant mantle was supported by higher-viscosity mantle at depth. Robinson and Parsons (1988) showed that this is a reasonable approximation if mantle viscosity increases sufficiently with depth. If this were not so, convective instability, which increases the rate of cooling of mantle columns, would cause more rapid seafloor subsidence rather than reduced subsidence as previously assumed (cf. O'Connell and Hager, 1980). The calculated geoid anomaly showed a rapid decline in the geoid–age slope as convective instability developed and comparing qualitatively with observed variations in geoid slope with age shown in **Figure 3**. Other more recent studies argue that convective motions that develop at young ages may explain depth and geoid–age data better than plate model advocates have assumed. Doin and Fleitout (1996) showed that a uniform heat flux supplied to the bottom of the thermal boundary layer, presumably by convective motions, explains depth–age, as well as a plate model, and also the rapid decline in the geoid–age slope at young ages.

Haxby and Weissel (1986) suggested the presence of longer wavelengths of small-scale convection beneath older regions of the Pacific. Wessel *et al.* (1996) identified gravity undulations with wavelengths of $\sim$280 and 1000 km that form small circles about the current pole of Pacific Plate motion. The shorter wavelengths would correspond to the Haxby gravity lineations. The longer wavelengths could reflect the spacing of hot-spot tracks or a larger scale of thermal boundary convective instability corresponding to that usually invoked to explain the plate model. The earlier study of Cazenave *et al.* (1995) had also indicated a wavelength of about 1000 km. Mantle seismic tomography using ray paths along a profile connecting Tonga and Hawaii identified seismic velocity anomalies with a spacing of about 1500 km that correlated with variations in gravity and bathymetry (Katzman *et al.*, 1998). As the depth of a convectively cooled mantle layer increases with time, simple dimensional and scaling arguments suggest that the wavelength of convective motions should increase, a behavior seen in early studies of convective instability (Buck and Parmentier, 1986), but more recent studies, summarized below, further address this.

The Haxby gravity lineations are subtle features of the gravity field, generally much smaller than gravity anomalies due to fracture zones, for example. Current Pacific and Nazca Plate motion is oblique to fracture zones so that lineations aligned with plate motion cut obliquely across them. For other plates that move nearly parallel to fracture zones within them, gravity lineations of comparable amplitude to those in the Pacific would be difficult to detect, so as to identify the possibility convective instability at young ages requires other evidence. If convective instability occurs beneath the fast moving Nazca and Pacific Plates created at the fast spreading EPR does it also occur beneath more slowly moving plates created by slower spreading? As discussed above, Sandwell and Schubert (1980) found that geoid height decreases approximately linearly with age for ages less than about 80 My for the Atlantic and southeast Indian spreading centers with geoid–age slopes comparable to that expected for purely conductive cooling, suggesting that small-scale convective instability at young ages does not occur beneath these more slowly spreading plates.

Previous studies have often treated either hot spots or small-scale convective instability as the mechanism of lithospheric heating in all ocean basins. However, one single mechanism of heat transfer need not be responsible for heating the lithosphere everywhere. With due caution concerning the nonlinearity of thermal convection (meaning that simply adding heat fluxes due to hot spots and small-scale convection may not be valid), it may even be reasonable to think that both mechanisms operate simultaneously but to different degrees beneath different ocean basins. Gravity lineations at young ages are visible only on the Pacific and Nazca Plates, suggesting that convective instability at young ages may develop under these fast moving plates. In the South Atlantic, where hot-spot tracks are sparse and gravity lineations are not detectable, root-age subsidence to ages exceeding 100 My would be consistent with purely conductive mantle cooling beneath this slower moving plate. Seafloor flattening at old ages in the North Atlantic could be due to heating by numerous hot spots.

7.07.2.7 Implications from Recent Theoretical and Experimental Studies of Convective Instability

Convective instability of a thermal boundary layer has been examined in numerous studies using a range of analytical methods (see for example, Yuen and Fleitout (1984) and Marquart *et al.* (1999)) as well as both laboratory and numerical experiments (*see* Chapters 7.03 and 7.05), the latter taking advantage of advances in computer speed and memory, to better understand the development of convective instability in a time-dependent basic state (conductive cooling) and temperature-dependent viscosity. The strong temperature dependence of mantle viscosity presents a significant challenge for numerical experiments and emphasizes the important continuing role of laboratory experiments. Davaille and Jaupart (1994) derived scaling laws for convective onset time (age) and heat flow in a viscous fluid with strongly temperature-dependent viscosity cooled from above.

A convective heat flux f independent of the depth of the convecting fluid, implying that the boundary thickness is small compared to the fluid depth, is given by

$$f = Ck\left(\frac{\rho\alpha g}{\mu\kappa}\right)^{1/3}\Delta T_c^{4/3}$$

where k, κ, α, and ρ are the thermal conductivity, thermal diffusivity, thermal expansion coefficient, and density, respectively, and $C = 0.16$ is a dimensionless constant determined from laboratory or numerical experiments. This expression for the heat flux follows directly from dimensional analysis. Davaille and Jaupart (1994) showed that the convecting thermal boundary layer coincided with a 10-fold increase in viscosity, corresponding to temperature decrease ΔT_c. For thermally activated creep

$$\mu = \mu_m \exp\left[\frac{Q}{R}\left(\frac{1}{T} - \frac{1}{T_m}\right)\right]$$

where μ_m and T_m correspond to the temperature and viscosity beneath the thermal boundary layer. Then

$$\Delta T_c = 2.24\frac{RT_m^2}{Q}$$

This heat flux scaling and the values of C is also confirmed by numerical experiments (Grasset and Parmentier, 1998). Heatflux as a function of μ_m and Q is shown in **Figure 6**. In the mantle, a heat flux due to small scale convection comparable to that which would be required by the plate model ($\sim$40 mW m^{-2}) and creep activation energies from $Q = 250$ to 600 kJ mol^{-1} would require asthenosphere viscosities between 3×10^{18} and 4×10^{17} Pa s.

The small scale of thermal structures and convective motions in the mantle predicted by laboratory and numerical experiments is important to appreciate. For a convective heat flux beneath old lithosphere of $\sim$40 mW m^{-2} and $\Delta T_c \sim 100°$C, the convecting thermal boundary layer thickness

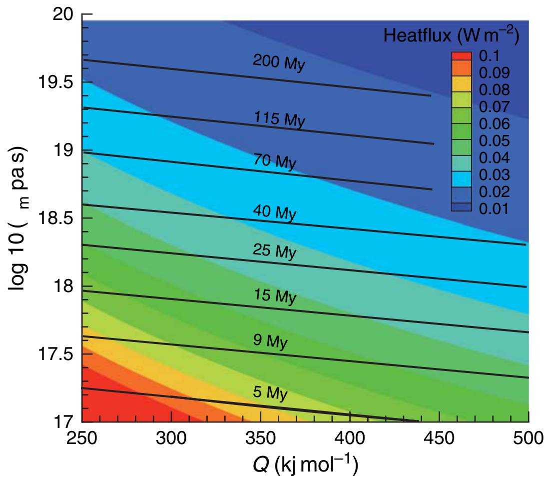

Figure 6 Contours of mantle heat flux beneath old oceanic lithosphere (based on heat flux scaling of Davaille and Jaupart (1994)) and onset time (age) of convective instability (from Zaranek and Parmentier, 2004) as a function of mantle viscosity and activation energy for thermally activated creep. For mantle heat flow below old oceanic crust of ~50 mW m^{-2} (see **Figure 2**), onset of convection at young ages should occur if the creep activation energy is sufficiently high and mantle viscosity sufficiently low.

$\delta_c \sim k\Delta T_c/f$ is less than 10 km, and convective instability of the boundary layer generates cold downwellings of comparable width.

The onset time of convective instability can also be determined from both laboratory and numerical experiments. For $Q = 250$ kJ mol^{-1} and a mantle temperature of 1300°C, Davaille and Jaupart predicted the onset time from their laboratory-derived scaling to be in the range 52–65 My. High-resolution numerical experiments examining the onset of convection in a fluid with strongly temperature-dependent viscosity have been reported in several recent studies (Huang *et al.*, 2003; Korenaga and Jordan, 2003a; Zaranek and Parmentier, 2004). These studies predict shorter onset times than earlier studies. Since convective motions, even those restricted to the upper mantle, must allow for scales as large as 1000 km, the small scales of convective instability indicated above would be difficult to resolve numerically. An understanding of the scaling of onset time with temperature dependence is needed to extrapolate well-resolved numerical experiments to the very stronger temperature dependences expected in the mantle. Recent numerical experiments, which are all in good agreement with each other, indicate a scaling for onset time that differed from that proposed by Davaille and Jaupart (2004). The onset time scaling of Zaranek and Parmentier (2004), for example, leads to the predictions shown in **Figure 6**.

In **Figure 6**, contours of heat flux provided to the base of the conductive lithosphere by small-scale convection in color shading and onset time in solid contours are plotted as a function of the creep activation energy Q and mantle viscosity μ_m beneath the thermal boundary layer. The upper-mantle viscosity mantle beneath spreading centers and other convectively active areas is not expected to exceed about 10^{19} Pa s (Bills, 1994; Passey, 1981; Sigmundsson, 1991). Estimates based on laboratory rheological measurements suggest an even lower viscosity of 10^{18} Pa s (Hirth and Kohlstedt, 1996). If small-scale convection provides all the heat flux to old seafloor (~45–50 mW m^{-2}, see **Figure 2**) and if an upper-mantle viscosity of 10^{18} Pa s is assumed, convective instability would occur at ages of ~15 My for $Q = 350$–400 kJ mol^{-1}, values intermediate between diffusion (~300 kJ mol^{-1}) and dislocation creep (~500 kJ mol^{-1}) in olivine.

The onset of convection at ages ≤10 My would require μ_m below 10^{18} Pa s and Q near the value for dislocation creep in olivine. For convective instability at 70 My with a convective heat flux of 40 mW m^{-2}, values of μ_m higher than those cited above would be required with a creep activation energy lower than 300 kJ mol^{-1}. For Q within the 300–500 kJ mol^{-1} range, onset of convection in the 50–70 My age range would be possible only with an upper-mantle viscosity of 10^{19} Pa s, and then only if the convective heat flux due to small-scale convection beneath old seafloor were ≤30 mW m^{-2}. This may be possible if small-scale convection transports only a fraction of the heat needed to explain the surface heatflow and bathymetry of old seafloor, the remainder being due to heating of the lithosphere at hot spots, as discussed earlier.

Mantle viscosity (μ_m introduced above) may differ near a spreading center and beneath older seafloor. Near spreading centers, the presence of melt may reduce viscosity. Conversely, since the presence of intragranular water in nominally anhydrous minerals reduces creep viscosity and water is a relatively incompatible element, the extraction of melt may dehydrate the mantle, thus increasing viscosity (Karato, 1986; Hirth and Kohlstedt, 1996). As discussed below, the latter effect may be the more dominant one, depending on the sensitivity of creep rates to water content and the water content of the mantle prior to melting.

As indicated above, convective instability at young ages may be present only beneath the Nazca and Pacific Plates, which are both fast moving and formed at a high spreading rate. Why might convective instability at young ages be restricted to fast spreading or fast moving plates? Is spreading rate or plate velocity the determining factor? Slower spreading rates should lead to a thicker thermal boundary layer beneath the spreading axis thus promoting convective instability at younger ages (Sparks and Parmentier, 1993). Other possible effects of spreading rate are discussed later. The linear stability analysis of Korenaga and Jordan (2003b) indicates that convective rolls aligned with plate motion may be stable only in the presence of strong shearing beneath fast moving plates. Rheological effects might also be important. Higher strain rates beneath fast moving plates could create smaller grain size resulting in more rapid diffusion creep or higher stresses resulting in deformation dominated by dislocation creep with higher Q. As shown in **Figure 6**, both effects would favor convective instability at younger ages. Rising mantle that is enriched in water relative to that in other regions might also explain a lower-mantle viscosity beneath the EPR, as discussed below, and promote early onset times.

The scale or wavelength of small-scale convection appears to increase to $\geq$1000 km beneath the old Pacific seafloor. Korenaga and Jordan (2004) recently examined how the horizontal scale of convective motions in a fluid with temperature and depth-dependent viscosity would increase with age, including in particular the effect of an endothermic phase transition at the base of the upper mantle. They suggested that convection initiated at small scales beneath moving plates could eventually penetrate the stable phase transition and evolve into whole-mantle convection.

All of the studies discussed above treat the development and evolution of convective motions as two-dimensional (2-D) and time dependent, most closely approximating convective motions in a vertical plane orthogonal to plate motion as a function of plate age. Despite significant advances in both digital technologies and numerical methodologies, fully 3-D treatments of thermal convection with the very strongly temperature-dependent viscosities believed to characterize mantle flow remain challenging. Numerical solutions must simultaneously resolve 10 km thick thermal boundary layer layers and cold plumes embedded in several thousand kilometer scale flow.

van Hunen *et al.* (2003) studied 3-D convective instability beneath a moving plate. In agreement with earlier analysis, plate motion enhanced the development of longitudinal convective rolls relative to motion-perpendicular transverse rolls. They found that the onset age of fully 3-D convective motions was similar to that in earlier 2-D studies. It would be interesting to more closely examine the evolution of convective motions with age, in particular how the scale convective motions increase as cooling proceeds. A first impression based on van Hunen *et al.* (2003, figure 1) suggests that the scale of convective motions does not increase as rapidly as suggested by earlier 2-D studies.

7.07.3 Convective Instability due to Melting in the Upper Mantle

7.07.3.1 Intraplate Volcanism as an Indicator of Upper-Mantle Convective Activity

Volcanism away from plate boundaries (*see* Chapters 1.13 and 7.09) is generally thought to be a consequence of decompression melting due to convective motions that arise from deeper in the mantle or from instability generated in the upper mantle. Linear, long-lived, and age-progressive volcanic chains have been explained as the manifestation of fixed hot spots, possibly generated by buoyant plumes of rising material originating deep in the mantle (Morgan, 1971). While the Wilson–Morgan fixed hot-spot model has been successfully applied to volcanic chains in all ocean basins, important disagreements have been recognized between geochronologic observations and the simplest predictions of the model. For example, Okal and Batiza (1987) and McNutt (1998) outline numerous examples where the fixed hot-spot model fails to explain: (1) observed departures from linearity of individual volcanic chains and inconsistent orientations among multiple chains which lie on the same plate, (2) short-lived chains and ones which fluctuate in size, and (3) violations of predicted along-chain age versus distance behavior. For example, the Cook–Austral Chain (Turner and Jarrard, 1982) and the Line Islands (Schlanger *et al.*, 1984), exhibit complex age progressions with volcanic activity occuring along multiple lineaments and with volcanoes of distinctly different ages in close proximity to one another. Furthermore, some linear volcanic ridges in the Pacific form much more rapidly than would be predicted by fixed hot-spot model (Bonatti *et al.*, 1977; Sandwell *et al.*, 1995).

The creation of large igneous provinces or oceanic plateaux by partial melting of the starting plume heads is a corollary of the mantle plume hypothesis for the origin of hot spots (Richards *et al.*, 1989). Of 14 possible Pacific hot-spot tracks studied by Clouard and Bonneville (2001), only three (Louisville, Easter, and Marquesas) can be traced to an oceanic plateau. Seven hot spots have short tracks <35 My and clearly cannot be traced to an oceanic plateau. Koppers *et al.* (2003) found that linear volcanic chains in the Western Pacific and South Pacific Superswell region typically display intermittent volcanic activity with longevities shorter than 40 My, superposed volcanism, and motion relative to other longer-lived hot spots. Finally, study of marine satellite gravity data in the Pacific (Wessel and Lyons, 1997) shows the presence of many volcanoes with a range of sizes in a variety of geologic settings. Most of these volcanoes do not clearly align in chains or ridges, and most seem too small to be explained by deep-mantle plumes. While the long-lived age progressive volcanic chains that fit the fixed hot-spot model are remarkable features, other mechanisms of intraplate volcanism must also be active.

7.07.3.2 Other Possible Mechanisms for Intraplate Volcanism

Diffuse plate extension (Sandwell *et al.*, 1995) has been frequently cited as a possible mechanism of intraplate volcanism. Proposed partly on morphological grounds, this mechanism was thought to explain rapid propagation of volcanic ridges and the formation of volcanic ridges in troughs of topography associated with the Haxby gravity lineations. Volcanism was thought to be attributable to either allowing melt already present in the upper mantle access to the surface or to decompression melting in upwellings associated with lithospheric boundinage. Dunbar and Sandwell (1988) calculated that 10% extension would be required for this mechanism. However, the amount of extension that can be allowed in the Pacific is less than 1% (Goodwillie and Parsons, 1992; Gans *et al.*, 2003), seemingly much too small for significant boudinage. Thus, agreement seems to be emerging that the boudinage hypothesis does not satisfy available observations. An interesting alternative is cracking of the lithosphere under the action of thermal contraction bending moments (Gans *et al.*, 2003; Sandwell and Fialko, 2004). In this hypothesis, cracking of the plate allows lithosphere between cracks to bend, thus relieving thermal bending moments. Cracks form topographic troughs, and magma already existing beneath the lithosphere exploits these regions to reach the seafloor. Mantle seismic velocities beneath volcanic ridges formed in this way should be higher than in adjacent mantle, which does not seem to be the case, at least beneath the few ridges where regional seismic data is available. Weeraratne *et al.* (2006) find lower seismic velocities, implying higher temperatures and/or more melt beneath ridges. However, the ridges examined in this study are all near the EPR spreading center on seafloor younger than 3 Ma. Seismic velocities beneath recently active volcanic ridges further from the spreading axis have not yet been studied in comparable ways.

7.07.3.3 Melting in Convectively Driven Upwellings

Volcanism due to decompression melting in small-scale convective upwellings is perhaps the favored popular hypothesis for the origin of volcanic ridges aligned with plate motion. Melting in convective upwellings would be consistent with lower seismic velocities in the mantle beneath ridges. Buoyant convective upwellings should elevate the seafloor so that the resulting volcanism should occur on topographic highs. However, volcanic ridges were observed to lie in lows of the gravity lineations. If gravity lows correspond to topographic troughs, this would be inconsistent with a convective origin (Sandwell *et al.*, 1995). However, seafloor topography with 100 m amplitudes over horizontal scales of several hundred kilometers are subtle features compared to the topography of volcanic constructs and the flexure caused by this loading. After removing lithospheric flexure due to the topographic loading, Harmon *et al.* (2006) found that volcanic ridges near the EPR actually lie on topographic highs. Topographic highs correspond to negative residual mantle Bouguer gravity anomalies which were obtained from the observed free air anomaly by subtracting the effect of crustal thickness variations and the attraction of topography. If this relationship holds for other volcanic ridges, particularly those further from the EPR axis, then a convective origin for volcanic ridges and gravity lineations would be indicated.

7.07.3.4 Buoyant Decompression Melting

In addition to decompression melting in thermally driven convection, intraplate volcanism may be a product of decompression melting in convective upwellings that result from the buoyancy associated with melting itself (Tackley and Stevenson, 1993; Raddick *et al.*, 2002; Hernlund and Tackley, 2003). This 'buoyant decompression melting' in a layer that is initially at its melting temperature may organize from small, initially random perturbations and thus might be termed 'magmatic convective storms'. Melt extraction leaves behind a buoyant and creep resistant residual mantle. The accumulation of this relatively immobile and infertile mantle ultimately limits the amount of melt that can be produced by the decompression melting mechanism (Raddick *et al.*, 2002). This results in an inverse correlation between the rate of melt production and the duration of melting, which may be diagnostic of the buoyant decompression melting process.

Buoyant decompression melting could occur in a number of geologic settings; however, if the oceanic upper mantle has previously melted beneath a spreading center and subsequently cooled, spontaneous buoyant decompression melting may be possible only in regions where a large-scale mantle upwelling can counteract conductive cooling, keeping the mantle at its solidus temperature over some depth range. The South Pacific Superswell has been interpreted as a region of large-scale mantle upwelling (McNutt, 1998; Gaboret *et al.*, 2003), and buoyant decompression melting may explain the abundance of volcanism associated with it. Alternatively, to balance the downward flux associated with sinking lithosphere, a small upward velocity should be present in large areas of the upper mantle away from convergent plate boundaries. Since transition zone mineral phases like the β- and γ-olivine have a larger water storage capacity than their lower pressure isomorph, upwelling mantle may dehydrate forming a water-rich melt above the transition zone. During the upward percolation of buoyant melt, as envisioned in an early study by Frank (1968), buoyant instabilities may lead to localization of melting, upwelling, and surface volcanism.

In the absence of a large-scale upwelling, where mantle is slightly cooler than its melting temperature, buoyant melting may not occur spontaneously but may be triggered by some initial upwelling due to relief on the bottom of the lithosphere, for example, across oceanic fracture zones that move obliquely across the mantle. This may provide a physical explanation for intraplate volcanism that is controlled by lithosphere structure.

7.07.4 Upwelling and Melting beneath Oceanic Spreading Centers

7.07.4.1 Melting, Melt Extraction, and the Chemical Lithosphere

Mantle upwelling and decompression melting beneath spreading centers is expected to have important consequences for the development of convective motions as the lithosphere ages. Two effects may be particularly important: (1) melting and melt extraction are expected to affect both rheology and density and (2) convective instability beneath the spreading axis due to density variations associated with the presence of melt and its extraction from residual mantle may influence the scale and evolution of off-axis convective instability. Forsyth (1992) provides a relatively recent review of mantle flow beneath spreading centers and the mantle electromagnetic and tomography (MELT) experiment (Forsyth *et al.*, 1998) provides the best geophysical evidence on the amount and distribution of melt in the mantle beneath a very fast spreading section of the EPR. Geochemistry provides evidence that garnet was present during melting, thus providing a minimum estimate of $\sim$70 km for the beginning of melting in upwelling mantle.

Hirth and Kohlstedt (1996) and Phipps Morgan (1997) pointed out that melting beneath spreading centers should produce a compositional lithosphere that is both more viscous, as mentioned above, and compositionally buoyant. Intragranular water that enhances the creep rate of nominally anhydrous mantle minerals behaves as a highly incompatible element during melting. The extraction of melt during fractional melting would leave behind a dry residual mantle. Removing essentially all the water present at concentrations inferred for upper mantle that melts beneath spreading centers may increase its viscosity by more than a factor of 100 (Hirth and Kohlstedt, 1996) (Chapter 2.14). The thickness of the residual layer should be comparable to the maximum depth of melting beneath a spreading center. Evans *et al.* (2005), using electrical conductivity, inferred a 60 km dehydration depth beneath a fast spreading section of the EPR (the MELT area at 17° S). The dehydrated residual mantle layer generated at a spreading center might be thought to correspond to the plate in the plate model seafloor evolution. However, this depth of dehydration appears significantly thinner than estimates of plate thickness in the range of 95–125 km discussed above. One possibility is that small amounts of wet melt form at the even greater depths comparable to the plate thickness. Interpretations of seismic data from the MELT experiment do suggest small amounts of melting at depths exceeding 100 km (Forsyth *et al.*, 1998).

7.07.4.2 Influence of Melt Extraction Mechanism

The rheological consequences of melt extraction should depend on the mechanism of melt migration. Does melt percolating upward remain distributed along mineral grain edges maintaining equilibrium with solid mantle as it goes? Or does it localize into larger channels after only small amounts of melt form? Melt that rapidly localizes into larger channels approximates ideal fractional melting which removes incompatible elements more effectively than equilibrium transport.

A fundamental observation is that the chemical composition of basalt erupted at spreading centers is not in equilibrium with residual mantle at low pressure (e.g., O'Hara, 1965; Stolper, 1980; Elthon and Scarfe, 1984). Melts must rise from depths of at least 30 km to the surface without extensive re-equilibration with surrounding mantle at shallow depth in order to preserve this deep geochemical signature. Focused melt flow through high permeability conduits or channels is one possible mechanism. Several lines of evidence suggest that the porosity structure in the melt generation and extraction region of the mantle is heterogeneous consisting of interconnected high-porosity dunite channels embedded in a low-porosity harzburgite or lherzolite matrix (Kelemen *et al.* (1997) and references therein). Remnant dunite channels have been observed as veins, tabular or sometimes irregular shaped bodies in ophiolites. These dunite dikes or veins make up 5–15% of the mantle in the Oman ophiolite with widths ranging from tens of millimeters to ~200 m and lengths from tens of meters to at least 10 km (Kelemen *et al.*, 1997). Although their spatial distribution in the mantle is still not well constrained, the presence of a high porosity, interconnected, coalescing network of dunite channels present above or within the melting region, has been envisioned. Porous flow through dunite channels is capable of producing observed Uranium-series disequilibria and significant trace element fractionations during mantle melting and melt extraction (e.g., Spiegelman and Elliot, 1993; Kelemen *et al.*, 1997; Spiegelman and Kelemen, 2003; Lundstrom, 2003).

At fast spreading rates, mantle upwelling and melting appear to occur over a several hundred kilometer wide region (e.g., Forsyth *et al.*, 1998) but the oceanic crust is emplaced within a few kilometers of the spreading axis. Thus, a second major constraint on the mechanism of melt migration is that it must be capable of focusing melt to the spreading axis. If the viscosity of upwelling mantle is sufficiently high ($\geq 10^{20}$ Pa s) pressure gradients in the mantle flow may be sufficient to drive melt to the spreading axis (Spiegelman and McKenzie, 1987; Phipps Morgan, 1987). Alternatively, melt may migrate vertically to collect in a decompaction boundary layer that develops as melt begins to freeze. This should create a high-porosity melt channel that slopes away from the spreading axis providing a conduit for melt flow toward the axis (Sparks and Parmentier, 1991; Spiegelman, 1993). Rabinowitz and Ceuleneer (2005) suggest, in fact, that dunites in the Oman ophiolite may be the preserved remnants of this decompaction boundary layer. If melt in the decompaction layer is isolated in dunite channels, then some signature of high pressures will be preserved in the melts that accumulate near the spreading axis. However, melting need not be perfectly fractional so that mantle need not be fully dehydrated.

No seismic or electromagnetic evidence on the distribution of melting and upwelling in the mantle comparable to that for southern EPR is available for slower spreading centers. If buoyancy related to melting is important, then 'active' upwelling could lead to more localized melting at slow spreading rates. Active upwelling would produce higher, more uniform degrees of melting creating more strongly and uniformly dehydrated residual mantle less prone to convective instability. This is illustrated in **Figure 7** from Braun *et al.* (2000).

7.07.4.3 2-D versus 3-D Upwelling and the Spreading Rate Dependence of Seafloor Structure

At slow spreading rates, buoyancy related to melting may also result in localized columns of upwelling and melting beneath the spreading axis (Parmentier and Phipps Morgan, 1990; Choblet and Parmentier, 2001). At high spreading rates, upwelling remains sheet like along the spreading axis. This is one possible

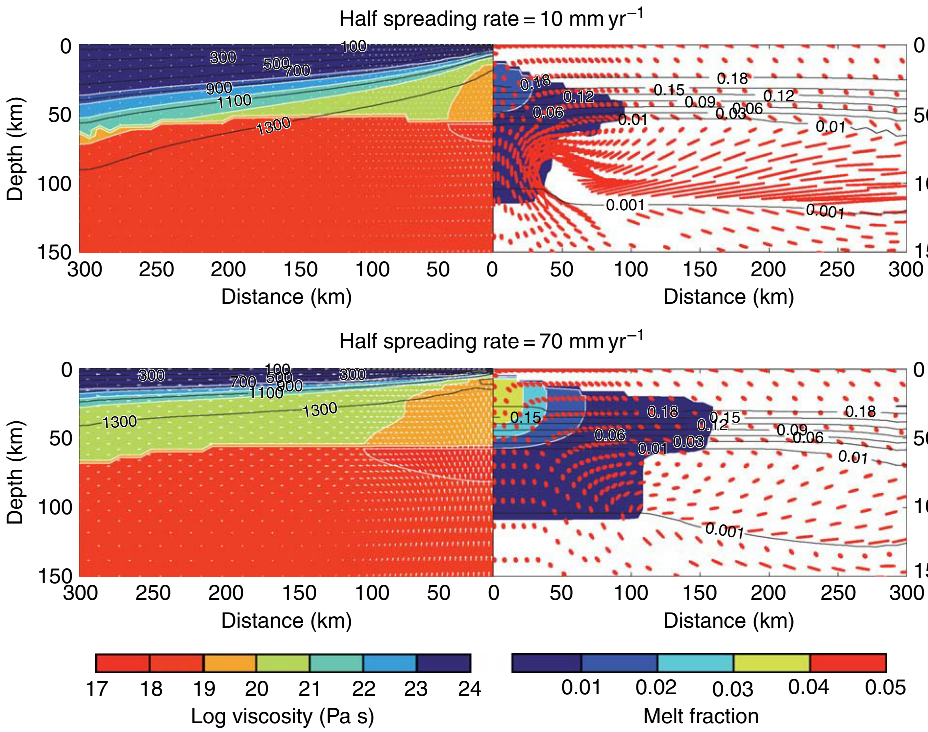

Figure 7 Mantle upwelling and melting beneath fast and slow spreading centers from Braun, *et al*. (2000). Solid contours in the left panel show the mantle viscosity, and black lines depict isotherms (at 200°C intervals) for a potential temperature of 1350°C and an adiabatic gradient of 0.3°C km^{-1}. Ellipses (red ovals) representing accumulated finite strain are plotted along solid flow streamlines corresponding to the velocity field shown by white vectors in the left panel. Solid contours on the right panel show the steady-state melt fraction (>0.1%) overlain by isodepletion contours (black lines). Rheology includes estimates of the effects of dehydration, melt, and grain boundary sliding with a reference viscosity of 5×10^{18} Pa s. Since the effects of dehydration dominate those of melt, the viscosity and velocity structures resemble more passive-like plate spreading flow above the dry solidus. Even with lower reference viscosities, buoyant flow is restricted to depths beneath the dry solidus. Buoyant localization of solid flow and melt generation at depth increases as the half-spreading rate decreases. The magnitude and localization of strain also increases with decreasing spreading rate.

explanation for the difference in seafloor morphology and structure between fast and slow spreading centers, and may also explain the strongly lineated morphology of seafloor produced at slow spreading rates (Phipps Morgan and Parmentier, 1995). At high spreading rates, buoyant decompression melting may produce off-axis upwelling columns that may explain near-axis volcanic ridges (Jha *et al*., 1997) providing a possible alternative to melting in thermally driven upwellings as discussed above.

7.07.5 Summary

The deviation of the age dependence of seafloor depth from predictions of a simple conductive thermal boundary layer (half-space cooling model) need not be explained by only a single mechanism. Both heating by hot spots and convective instability due to cooling from above may affect thermal evolution but differ in importance in different settings, for example, the North Atlantic and Pacific, respectively. Discussion has sometimes focused on which mechanism is the correct one rather than on assessing which may be more important and why. The relative importance of convective instability should depend on spreading rate and mantle composition, perhaps particularly through the effect of water on rheology.

The seafloor age at which convective instability begins clearly depends strongly on spreading rate and particularly mantle rheology. Convective instability at young ages remains a preferred explanation for gravity lineations on the Pacific and Nazca Plates, but is not required beneath other plates. Beneath thicker, colder lithosphere at slow spreading centers, small-scale convection may be present but less visible. If small-scale convection is present beneath the fast spreading EPR but not beneath slower spreading centers, a number of explanations for this possible difference in behavior can be envisioned. The higher shear rates beneath rapid moving plates may organize convection into a lineated structure that is more visible in gravity data than other less-organized patterns. Higher shear rates may also result in lower effective viscosity of the upper mantle beneath faster moving plates; therefore yielding earlier onset times.

Intraplate volcanism not associated with hot spots on Pacific and Nazca Plates is much more abundant than in other ocean basins. Does this reflect an influence of deeper-mantle processes or convective instability that develops within the upper mantle? The latter possibility would be broadly consistent with a lower-viscosity (higher strain rate, smaller grain size, and/or wetter) mantle beneath the Pacific and Nazca Plates than elsewhere in the upper mantle.

References

Bergman EA and Solomon SC (1984) Source mechanisms of earthquakes near mid-ocean ridges from body waveform inversion; implications for the early evolution of oceanic lithosphere. *Journal of Geophysical Research* 89: 11415–11441.

Bills BG (1994) Viscosity estimates for the crust and upper mantle from patterns of lacustrine shoreline deformation in the eastern Great Basin. *Journal of Geophysical Research* 99: 22059–22086.

Bonatti E, Harrison CGA, Fisher DE, *et al.* (1977) Easter volcanic chain (southeast Pacific): A mantle hotline. *Journal of Geophysical Research* 82: 2437–2478.

Braun M, Hirth G, and Parmentier EM (2000) Effects of deep damp melting on mantle flow and melt generation beneath mid-ocean ridges. *Earth and Planetary Science Letters* 176: 339–356.

Buck WR (1985) When does small scale convection begin beneath oceanic lithosphere? *Nature* 313: 775–777.

Buck WR (1987) Analysis of the cooling of a variable-viscosity fluid with applications to the Earth. *Geophysical Journal of the Royal Astronomical Society* 89: 549–577.

Buck WR and Parmentier EM (1986) Convection beneath young oceanic lithosphere: Implications for thermal structure and gravity. *Journal of Geophysical Research* 91: 1961–1974.

Carlson RL and Johnson HP (1994) On modeling the thermal evolution of the oceanic upper mantle: An assessment of the cooling plate model. *Journal of Geophysical Research* 99: 3201–3214 (doi: 10.1029/93JB02696).

Cazenave A (1984) Thermal cooling of the oceanic lithosphere: New constraints from geoid height data. *Earth and Planetary Science Letters* 70: 395–406.

Cazenave A, Lago B, and Dominh K (1982) Geoid anomalies over the north-east Pacific fracture zones from satellite altimeter data. *Geophysical Journal* 69: 15–31.

Cazenave A, Lago B, and Dominh K (1983) Thermal parameters of the oceanic lithosphere estimated from geoid height data. *Journal of Geophysical Research* 88: 1105–1118.

Cazenave A, Parsons B, and Calcagno P (1995) Geoid lineations of 1000-km wavelength over the central Pacific. *Geophysical Research Letters* 22: 97–100.

Chase CG (1985) The geological significance of the geoid. *Annual Review of Earth and Planetary Sciences* 13: 97–117.

Chastel YB, Dawson PR, Wenk H-R, and Bennett K (1993) Anisotropic convection with implications for the upper mantle. *Journal of Geophysical Research* 98: 17757–17772 (doi:10.1029/93JB01161).

Choblet G and Parmentier EM (2001) Mantle upwelling and melting beneath slow spreading centers: Effects of variable rheology and melt productivity. *Earth and Planetary Science Letters* 184: 589–604.

Clouard V and Bonneville A (2001) How many Pacific hotspots are fed by deep-mantle plumes? *Geology* 29: 695–698.

Colin P and Fleitout L (1990) Topography of the ocean floor: Thermal evolution of the lithosphere and interaction of the deep mantle heterogeneities with the lithosphere. *Geophysical Research Letters* 17: 1961–1964.

Craig CH and McKenzie DP (1986) The existence of a thin low-viscosity layer beneath the lithosphere. *Earth and Planetary Science Letters* 78: 420–426.

Crough ST (1978) Thermal origin of mid-plate hot-spot swells. *Geophysical Journal of the Royal Astronomical Society* 55: 451–469.

Crough ST (1975) Thermal model of oceanic lithosphere. *Nature* 256: 388–390.

Crough ST (1977) Approximate solutions for the formation of the lithosphere. *Earth and Planetary Science Letters* 14: 365–377.

Crough ST (1979a) Geoid anomalies across fracture zones and the thickness of the lithosphere. *Earth and Planetary Science Letters* 44: 224–230.

Crough ST (1979b) Hotspot epeirogeny. *Tectonophysics* 61: 321–333.

Davaille A and Jaupart C (1994) One onset of thermal convection in fluids with temperature-dependent viscosity: Application to the ocean mantle. *Journal of Geophysical Research* 99: 19853–19866.

Davis EE and Lister CRB (1974) Fundamentals of ridge crest topography. *Earth and Planetary Science Letters* 21: 405–413.

Davis EE, Lister CRB, and Sclater JG (1984) Towards determining the thermal state of the thermal state of old oceanic lithosphere; heat flow measurements from the Blake-Bahama outer ridge, northwestern Atlantic. *Geophysical Journal of the Royal Astronomical Society* 78: 707–1545.

Detrick RS (1981) An analysis of geoid anomalies across the Mendocino fracture zone: Implications for thermal models of the lithosphere. *Journal of Geophysical Research* 86: 11751–11762.

Detrick RS and Crough ST (1978) Island subsidence, hot spots and lithosphere thinning. *Journal of Geophysical Research* 83: 1236–1244.

Doin MP and Fleitout L (1996) Thermal evolution of the oceanic lithosphere: An alternative view. *Earth and Planetary Science Letters* 142: 121–136.

Doin M-P, Fleitout L, and McKenzie D (1996) Geoid anomalies and the structure of continental and oceanic lithospheres. *Journal of Geophysical Research* 101: 16119–16136 (doi:10.1029/96JB00640).

Driscoll ML and Parsons B (1988) Cooling of the oceanic lithosphere – evidence from geoid anomalies across the Udintsev and Eltanin fracture zones. *Earth and Planetary Science Letters* 88: 289–307.

Dunbar J and Sandwell D (1988) A boudinage model for cross-grain lineations (abs.). *EOS Transactions of the American Geophysical Union* 69: 1429.

Eberle MA and Forsyth DW (1995) Regional viscosity variations, small-scale convection and the slope of the depth–age $\frac{1}{2}$ curve. *Geophysical Research Letters* 22: 473–476.

Ekstrom G and Dziewonski AM (1998) The unique anisotropy of the Pacific upper mantle. *Nature* 394: 168–172.

Elthon D and Scarfe CM (1984) High-pressure phase equilibria of a high-magnesia basalt and the genesis of primary oceanic basalts. *American Mineralogist* 69: 1–15.

Evans RL, Hirth G, Baba K, Forsyth D, Chave A, and Mackie R (2005) Geophysical evidence from the MELT area for compositional controls on oceanic plates. *Nature* 437: 249–252.

Faul U and Jackson I (2005) The seismological signature of temperature and grain size variations in the upper mantle. *Earth and Planetary Science Letters* 234: 119–234.

Fleitiout L and Yuen DA (1984) Secondary convection and the growth of the oceanic lithosphere. *Physics of the Earth and Planetary Interiors* 36: 181–212.

Fleitout L and Moriceau C (1992) Short-wavelength geoid, bathymetry and convective pattern beneath the Pacific Ocean. *Geophysical Journal International* 110: 6–28.

Forsyth DW (1992) Geophysical constraints on mantle flow and melt generation beneath mid-ocean ridges. In: Phipps MJ, Blackman DK, and Sinton JM (eds.) *Geophysical Monograph Series 71: Evolution of Mid Ocean Ridges*, pp. 1–66. Washington, DC: American Geophysical Union.

Forsyth DW, and The MELT Seismic Team (1998) Imaging the deep seismic structure beneath a mid-ocean ridge: The MELT experiment. *Science* 280: 1215–1218.

Frank FC (1968) Two component model for convection in the Earth's upper mantle. *Nature* 220: 350–352.

Freedman AP and Parsons B (1990) Geoid anomalies over two South Atlantic fracture zones. *Earth and Planetary Science Letters* 100: 18–41.

Gaboret C, Forte AM, and Montagner JP (2003) The unique dynamics of the Pacific hemisphere mantle and its signature on seismic anisotropy. *Earth and Planetary Science Letters* 208: 219–233.

Gans KD, Wilson DS, and Macdonald KC (2003) Pacific plate gravity lineaments: Diffuse extension or thermal contraction? *Geochemistry Geophysics Geosystems* 4(9): 1074 (doi:10.1029/2002GC000465).

Goodwillie AM and Parsons B (1992) Placing bounds on lithospheric deformation in the central Pacific Ocean. *Earth and Planetary Science Letters* 111: 123–139.

Grasset O and Parmentier EM (1998) Thermal convection in a volumetrically heated, infinite Prandtl number fluid with strongly temperature-dependent viscosity: Implications for planetary thermal evolution. *Journal of Geophysical Research* 103: 18171–18181.

Gribb TT and Cooper RF (1998) Low-frequency shear wave attenuation in polycrystalline olivine: Grain boundary diffusion and the physical significance of the Andrade model for viscoelastic rheology. *Journal of Geophysical Research* 103: 27267–27279.

Harmon N, Forsyth DW, and Scheirer DS (2006) Analysis of gravity and topography in the GLIMPSE study region: Isostatic compensation and uplift of the Sojourn and Hotu Matua Ridge systems. *Journal of Geophysical Research* 111: B11406 (doi: 10.1029/2005JB004071).

Haxby WF and Turcotte DL (1978) Isostatic geoid anomalies. *Journal of Geophysical Research* 83: 5473–5478.

Haxby WF and Weissel JK (1986) Evidence for small scale convection for SEASAT altimeter data. *Journal of Geophysical Research* 91: 3507–3520.

Hayes DE (1988) Age-depth relationships and depth anomalies in the southeast Indian Ocean and south Atlantic Ocean. *Journal of Geophysical Research* 93: 2937–2954.

Heestand RL and Crough ST (1981) The effect of hot spots on the oceanic age-depth relation. *Journal of Geophysical Research* 86: 6107–6114.

Hernlund JW and Tackley PJ (2003) Post-laramide volcanism and upper mantle dynamics in the Western US: Role of small-scale convection, *Eos Transactions AGU*, Fall Meeting Supplement 84(46):, Abstract V31F-07.

Hirth G, Evans RL, and Chave AD (2000) Comparison of continental and oceanic mantle electrical conductivity: Is the Archean lithosphere dry? *Geochemistry Geophysics Geosystems* 1: (doi:10.1029/2000GC000048).

Hirth G and Kohlstedt DL (1996) Water in the oceanic upper mantle: Implications for rheology, melt extraction, and the evolution of the lithosphere. *Earth and Planetary Science Letters* 144: 93–108.

Huang J and Zhong S (2005) Sublithospheric small-scale convection and its implications for the residual topography at old ocean basins and the plate model. *Journal of Geophysical Research* 110: B05404 (doi:10.1029/2004JB003153).

Huang J, Zhong S, and van Hunen J (2003) Controls on sublithospheric small-scale convection. *Journal of Geophysical Research* 108: 2405 (doi:10.1029/2003JB002456).

Jha K, Parmentier EM, and Sparks DW (1997) Buoyant mantle upwelling and crustal production at oceanic spreading centers: On-axis segmentation and off-axis melting. *Journal of Geophysical Research* 102: 11979–11989.

Johnson HP and Carlson RL (1992) Variation of sea floor depth with age: A test of model based on drilling results. *Geophysical Research Letters* 19: 1971–1974.

Kaminski É and Ribe NM (2001) A kinematic model for recrystallization and texture development in olivine polycrystals. *Earth and Planetetary Science Letters* 189: 253–267.

Kaminski É and Ribe NM (2002) Timescales for the evolution of seismic anisotropy in mantle flow. *Geochemistry Geophysics Geosystems* 3: (doi:10.1029/2001GC000222).

Karato S (1986) Does partial melting reduce the creep strength of the upper mantle. *Nature* 319: 309–310.

Katzman R, Zhao L, and Jordan TH (1998) High-resolution, two-dimensional vertical tomography of the central Pacific mantle using ScS reverberations and frequency-dependent travel times. *Journal of Geophysical Research* 103: 17933–17972 (doi:10.1029/98JB00504).

Kelemen PB, Hirth G, Shimizu N, Spiegelman M, and Dick HJB (1997) A review of melt migration processes in the adiabatically upwelling mantle beneath oceanic spreading ridges. *Philosophical Transactions of the Royal Society of London A* 355: 282–318.

Koppers AAP, Staudigel H, Pringle MS, and Wijbrans JR (2003) Short-lived and discontinuous intraplate volcanism in the south Pacific: Hot spots or extensional volcanism? *Geochemistry Geophysics Geosystems* 4: 1089 (doi:10.1029/2003GC000533).

Korenaga J and Jordan TH (2003a) Linear stability analysis of Richter rolls. *Geophysical Research Letters* 30(22): 2157 (doi:10.1029/2003GL018337).

Korenaga J and Jordan TH (2003b) Physics of multiscale convection in Earth's mantle: Onset of sublithospheric convection. *Journal of Geophysical Research* 108: 2333 (doi:10.1029/2002JB001760).

Korenaga J and Jordan TH (2004) Physics of multiscale convection in Earth's mantle: Evolution of sublithospheric convection. *Journal of Geophysical Research* 109: B01405 (doi:10.1029/2003JB002464).

Langseth MG, LePichon X, and Ewing M (1966) Crustal structure of mid-ocean ridges. Part 5: Heat flow through the Atlantic Ocean and convection currents. *Journal of Geophysical Research* 71: 5321–5355.

Lawrence JF and Shearer PM (2006) A global study of transition zone thickness using receiver functions. *Journal of Geophysical Research* 111: B06307 (doi:10.1029/2005JB003973).

Levitt DA and Sandwell DT (1995) Lithospheric bending at subduction zones based on depth soundings and satellite gravity. *Journal of Geophysical Research* 100: 379–400.

Lin J and Parmentier EM (1985) Surface topography due to convection in a variable viscosity fluid: Application to short wavelength gravity anomalies in the central Pacific Ocean. *Geophysical Research Letters* 12: 357–360.

Lister CRB, Sclater JG, Davis EE, Villinger H, and Nagihara S (1990) Heat flow maintained in ocean basins of great age: Investigations in the north-equatorial west Pacific. *Geophysical Journal International* 102: 603–630.

Lizarralde D, Chave A, Hirth G, and Schultz A (1995) Northeastern Pacific mantle conductivity profile from long-period magnetotelluric sounding using Hawaii-to-California submarine cable data. *Journal of Geophysical Research* 100: 17837–17854.

Lundstrom CC (2003) Uranium-series disequilibria in mid-ocean ridge basalts: Observations and models of basalt genesis. In: Bourdon B, Henderson GM, Lundstrom CC, and Turner SP (eds.) *Reviews in Mineralogy and Geochemistry 52: Uranium-Series Geochemistry*, pp. 175–214. Chantilly, VA: Mineralogical Society of America.

Lynch MA (1999) Linear ridge groups: evidence for tensional cracking in the Pacific Plate. *Journal of Geophysical Research* 104: 29321–29333.

Maggi A, Debayle E, Priestly K, and Barruol G (2006) Multimode surface waveform tomography of the Pacific ocean: A close look at the lithospheric cooling signature. *Geophysical Journal International* 166: 1384–1397.

Marquart G, Schmelling H, and Braun A (1999) Small-scale instabilities below the cooling oceanic lithosphere. *Geophysical Journal International* 138: 655–666.

Marty J-C and Casanave A (1989) Regional variations in subsidence rate of oceanic plates: A global analysis. *Earth and Planetary Science Letters* 94: 301–315.

Marty J-C and Cazenave A (1988) Thermal evolution of the lithosphere beneath fracture zones inferred from geoid anomalies. *Geophysical Research Letters* 15: 593–596.

Marty J-C, Cazenave A, and Lago B (1988) Geoid anomalies across Pacific fracture zones. *Geophysical Journal* 93: 1–23.

McKenzie DP (1967) Some remarks on heat flow and gravity anomalies. *Journal of Geophysical Research* 72: 6261–6273.

McKenzie DP and Sclater JG (1969) Heat flow in the eastern Pacific and sea-floor spreading. *Bulletin of Volcanology* 33: 101–118.

McNutt MK (1998) Superswells. *Reviews of Geophysics* 36: 211–244.

Morgan WJ (1968) Rises, trenches, great faults, and crustal blocks. *Journal of Geophysical Research* 73: 1959.

Morgan WJ (1971) Convection plumes in the lower mantle. *Nature* 230: 42–43.

Morgan WJ (1972) Deep mantle convection plumes and plate motions. *American Association of Petroleum Geologist Bulletin* 56: 203–213.

Nagihara S, Lister CRB, and Sclater JG (1996) Reheating of old oceanic lithosphere: Deductions from observations. *Earth and Planetary Science Letters* 139: 91–104.

Nishimura CE and Forsyth DW (1989) The anisotropic structure of the upper mantle in the Pacific. *Geophysical Journal* 96: 203–229.

O'Connell RJ and Hager BH (1980) On the thermal state of the Earth. In: Dziewonski A and Boschi E (eds.) *Physics of the Earth's Interior*, pp. 270–317. Amsterdam: Elsevier.

O'Hara MJ (1965) Primary magmas and the origin of basalts. *Scottish Journal of Geology* 1: 19–40.

Okal EA and Batiza R (1987) Hotspots: The first 25 years. In: Keating BH, Fryer P, Batiza R, and Boehlert GW (eds.) *Seamounts, Islands, and Atolls*, pp. 1–11, Geophysical Monograph 43. Washington, DC: AGU.

Parmentier EM and Haxby WF (1986) Thermal stresses in the oceanic lithosphere: Evidence from geoid anomalies at fracture zones. *Journal of Geophysical Research* 91: 7193–7204.

Parmentier EM and Phipps MJ (1990) The spreading rate dependence of three-dimensional oceanic spreading center structure. *Nature* 348: 325–328.

Parsons B and McKenzie D (1978) Mantle convection and the thermal structure of the plates. *Journal of Geophysical Research* 83: 4485–4496.

Parsons B and Sclater JG (1977) An analysis of the variation of ocean floor bathymetry and heat flow with age. *Journal of Geophysical Research* 82: 803–827.

Passey QR (1981) Upper mantle viscosity derived from the difference in rebound of the Provo and Bonneville shorelines; Lake Bonneville Basin, Utah. *Journal of Geophysical Research* 86: 11701–11708.

Phipps MJ (1987) Melt migration beneath mid-ocean spreading centers. *Geophysical Research Letters* 14: 1238–1241.

Phipps MJ (1997) The generation of a compositional lithosphere by mid-ocean ridge melting and its effect on subsequent off-axis hotspot upwelling and melting. *Earth and Planetary Science Letters* 146: 213–232.

Phipps MJ and Parmentier EM (1995) Crenulated seafloor: Evidence for spreading rate dependent structure of mantle upwelling and melting beneath a mid-oceanic spreading center. *Earth and Planetary Science Letters* 129: 73–84.

Priestley D and McKenzie DM (2006) The thermal structure of the lithosphere from shear velocities. *Earth and Planetary Science Letters* 244: 285–301.

Rabinowicz M and Ceuleneer G (2005) The effect of sloped isotherms on melt flow in the shallow mantle: a physical and numerical model based on observations in the Oman ophiolite. *Earth and Planetary Science Letters* 229: 231–246.

Raddick MJ, Parmentier EM, and Scheirer DS (2002) Buoyant decompression melting: A possible mechanism for intraplate volcanism. *Journal of Geophysical Research* 107(B10): 2228 (doi:10.1029/2001JB000617).

Renkin ML and Sclater JG (1988) Depth and age in the North Pacific. *Journal of Geophysical Research* 93: 2910–2935.

Richards MA, Duncan RA, and Vincent EC (1989) Flood basalts and hot-spot tracks: Plume heads and tails. *Science* 246: 103–107.

Richter FM (1973) Convection and the large scale circulation of the mantle. *Journal of Geophysical Research* 74: 8735–8745.

Richter FM and Parsons B (1975) On the interaction of two scales of convection in the mantle. *Journal of Geophysical Research* 80: 2529–2541.

Ritzwoller MH, Shapiro NM, and Zhong S (2004) Cooling history of the Pacific lithosphere. *Earth and Planetary Science Letters* 226: 69–84.

Robinson EM and Parsons B (1988) Effect of a shallow low-viscosity zone on small-scale instabilities under the cooling oceanic plates. *Journal of Geophysical Research* 93: 3469–3479.

Sandwell DT (1984) Thermomechanical evolution of oceanic fracture zones. *Journal of Geophysical Research* 89: 11401–11413.

Sandwell DT and McAdoo DC (1988) Marine gravity of the southern ocean and Antarctic margin from Geosat. *Journal of Geophysical Research* 93: 10389–10396.

Sandwell D and Fialko Y (2004) Warping and cracking of the Pacific plate by thermal contraction. *Journal of Geophysical Research* 109: B10411 (doi:10.1029/2004JB003091).

Sandwell D and Schubert G (1980) Geoid height versus age for symmetric spreading ridges. *Journal of Geophysical Research* 85: 7235–7241.

Sandwell DT and Schubert G (1982a) Geoid height-age relation from SEASAT altimeter profiles across the Mendocino

fracture zone. *Journal of Geophysical Research* 87: 3949–3958.
Sandwell DT and Schubert G (1982b) Lithospheric flexure at fracture zones. *Journal of Geophysical Research* 87: 4657–4667.
Sandwell DT and Smith WHF (1997) Marine gravity anomaly from Geosat and ERS 1 satellite altimetry. *Journal of Geophysical Research* 102: 10039–10054 (doi:10.1029/96JB03223).
Sandwell DT, Winterer EL, Mammerickx J, *et al.* (1995) Evidence for diffuse extension of the Pacific plate from PukaPuka Ridges and Cross-Grain gravity lineations. *Journal of Geophysical Research* 100: 15087–15099.
Schlanger SO, Garcia MO, Keating BH, *et al.* (1984) Geology and geochronology of the Line Islands. *Journal of Geophysical Research* 89: 11261–11272.
Schroeder W (1984) The empirical age-depth relation and depth anomalies in the Pacific Ocean. *Journal of Geophysical Research* 89: 9873–9884.
Schubert G, Froidevaux C, and Yuen DA (1976) Oceanic lithosphere and asthenosphere: Thermal and mechanical structure. *Journal of Geophysical Research* 81: 3525–3540.
Schubert G and Turcotte DL (1972) One dimensional model of shallow mantle convection. *Journal of Geophysical Research* 77: 945–951.
Schubert G, Yuen DA, Froidevaux C, Fleitout L, and Souriau M (1978) Mantle circulation with partial shallow return flow. *Journal of Geophysical Research* 83: 745–758.
Sclater JG, Lawver LA, and Parsons B (1975) Comparison of long-wavelength residual elevation and free air gravity anomalies in the north Atlantic and possible implications for thickness of the lithosperic plate. *Journal of Geophysical Research* 80: 1031–1052.
Sigmundsson F (1991) Post-glacial rebound and asthenosphere viscosity in Iceland. *Geophysical Research Letters* 18: 1131–1134 (doi:10.1029/91GL01342).
Sleep NH (1969) Sensitivity of heat flow and gravity to the mechanism of seafloor spreading. *Journal of Geophysical Research* 74: 542–549.
Smith WHF (1998) Seafloor tectonic fabric from satellite altimetry. *Annual Review of Earth and Planetary Science* 26: 697–738.
Sparks DW and Parmentier EM (1991) Melt extraction from the mantle beneath spreading centers. *Earth and Planetary Science Letters* 105: 368–377.
Sparks DW and Parmentier EM (1993) The structure of three-dimensional convection beneath spreading centers. *Geophysical Jounal International* 112: 81–91.
Spiegelman M (1993) Physics of melt extraction: Theory, implications and applications. *Philosophical Transactions of the Royal Society of London A* 342: 23–41.
Spiegelman M and Elliot T (1993) Consequences of melt transport for Uranium series disequilibrium. *Earth and Planetary Science Letters* 118: 1–20.
Spiegelman M and Kelemen PB (2003) Extreme chemical variability as a consequence of channelized melt transport. *Geochemistry Geophysics Geosystems* 4(7): 1055 (doi: 1029/2002GC000336).
Spiegelman M and McKenzie D (1987) Simple 2-D models for melt extraction at mid-ocean ridges and island arcs. *Earth and Planetary Science Letters* 83: 137–152.
Stein CA and Stein S (1992) A model for the global variation in oceanic depth and heat flow with lithospheric age. *Nature* 359: 123–129.
Stein CA and Stein S (1993) Contraints on Pacific midplate swells from global depth–age and heat flow-age models. In: Pringle MS, Sager WW, Sliter WV, and Stein S (eds.) *Geophysical Monograph Series, vol. 77: The Mesozoic Pacific: Geology, Tectonics, and Volcanism*, pp. 53–76. Washinhton, DC: AGU.
Stixrude L and Lithgow-Bertelloni C (2005) Mineralogy and elasticity of the oceanic upper mantle: origin of the low-velocity zone. *Journal of Geophysical Research* 110: B03204 (doi:10.1029/2004JB002965).
Stolper E (1980) A phase diagram for mid-ocean ridge basalts: Preliminary results and implications for petrogenesis. *Contributions to Mineralogy and Petrology* 74: 13–27.
Tackley PJ and Stevenson DJ (1993) A mechanism for spontaneous self-perpetuating volcanism on the terrestrial planets. In: Stone DB and Runcorn SK (eds.) *Flow and Creep in the Solar System: Observations, Modeling and Theory*, pp. 307–321. Norwell, MA: Kluwer.
Turcotte DL and Oxburgh ER (1967) Finite amplitude convective cells and continental drift. *Journal of Fluid Mechanics* 28: 24–42.
Turner DL and Jarrard RD (1982) K-Ar dating of the Cook-Austral island chain: A test of the hot-spot hypothesis. *Journal of Volcanology and Geothermal Research* 12: 187–220.
van Hunen J, Huang J, and Zhong S (2003) The effect of shearing on the onset and vigor of small-scale convection in a Newtonian rheology. *Geophysical Research Letters* 30(19): 1991 (doi:10.1029/2003GL018101).
Vogt PR and Ostenso NA (1967) Steady state crustal spreading. *Nature* 215: 811–817.
Wang D, Mookerjee M, Xu Y, and Karato S (2006) The effect of water on the electrical conductivity of olivine. *Nature* 443: 977–980 (doi:10.1038/nature05256).
Wenk H-R and Tomé CN (1999) Modeling dynamic recrystallization of olivine aggregates deformed in simple shear. *Journal of Geophysical Research* 104: 25513–25528 (doi:10.1029/1999JB900261).
Weeraratne DS, Forsyth DW, Yang Y, and Webb SC (2007) Rayleigh wave tomography beneath intraplate volcanic ridges in the South Pacific. *Journal of Geophysical Research* 112: B06303 (doi: 10.1029/2006JB004403).
Wessel P (2001) Global distribution of seamounts inferred from gridded Geosat/ERS-1 altimetry. *Journal of Geophysical Research* 106: 19431–19441.
Wessel P and Haxby WF (1990) Thermal-stresses, differential subsidence, and flexure at oceanic fracture zones. *Journal of Geophysical Research* 95: 375–391.
Wessel P, Kroenke LW, and Bercovici D (1996) Pacific Plate motion and undulations in geoid and bathymetry. *Earth and Planetary Science Letters* 140: 53–66.
Wessel P and Lyons S (1997) Distribution of large Pacific seamounts from Geosat/ERS-1: Implications for the history of intraplate volcanism. *Journal of Geophysical Research* 102: 22459–22475.
Wiens DA and Stein S (1983) Age dependence of oceanic intraplate seismicity and implications for lithospheric evolution. *Journal of Geophysical Research* 88: 6455–6468.
Yoshino T, Matsuzaki T, Yamashita S, and Katsura T (2006) Hydrous olivine unable to account for conductivity anomaly at the top of the asthenosphere. *Nature* 443: 973–976 (doi:10.1038/nature05223).
Yuen DA and Fleitout L (1984) Stability of the oceanic lithosphere with variable viscosity: An initial-value approach. *Physics of the Earth and Planetary Interiors* 343: 173–185.
Zaranek SE and Parmentier EM (2004) Convective instability of a fluid with temperature-dependent viscosity cooled from above. *Earth and Planetary Science Letters* 224: 371–386.
Zhou Y, Nolet G, Dahlen FA, and Laske G (2006) Global upper-mantle structure from finite-frequency surface-wave tomography. *Journal of Geophysical Research* 111: B04304 (doi:10.1029/2005JB003677).